



Published in final edited form as:

Angiogenesis. 2015 April ; 18(2): 151–162. doi:10.1007/s10456-014-9453-2.

AKT hyper-phosphorylation associated with PI3K mutations in lymphatic endothelial cells from a patient with lymphatic malformation

Elisa Boscolo^{1,2}, Silvia Coma¹, Valerie L. Luks³, Arin Greene⁴, Michael Klagsbrun¹, Matthew L. Warman³, and Joyce Bischoff¹

¹Vascular Biology Program and Department of Surgery, Boston Children's Hospital, Harvard Medical School, MA, USA

³Departments of Orthopedic Surgery and Genetics and the Vascular Anomalies Center, Boston Children's Hospital, Harvard Medical School, MA USA

⁴Department of Plastic and Oral Surgery and Vascular Anomalies Center, Boston Children's Hospital and Harvard Medical School, MA USA

Abstract

Lymphatic malformations (LM) are characterized by abnormal formation of lymphatic vessels and tissue overgrowth. The lymphatic vessels present in LM lesions may become blocked and enlarged as lymphatic fluid collects, forming a mass or cyst. Lesions are typically diagnosed during childhood, and are often disfiguring and life threatening. Available treatments consist of sclerotherapy, surgical removal and therapies to diminish complications.

We isolated lymphatic endothelial cells (LM-LEC) from a surgically removed microcystic LM lesion. LM-LEC and normal human dermal-LEC (HD-LEC) expressed endothelial (CD31, VE-Cadherin) as well as lymphatic endothelial (Podoplanin, PROX1, LYVE1)-specific markers. Targeted gene sequencing analysis in patient-derived LM-LEC revealed the presence of two mutations in class I phosphoinositide 3-kinases (PI3K) genes. One is an inherited, premature stop codon in the PI3K regulatory subunit *PIK3R3*. The second is a somatic missense mutation in the PI3K catalytic subunit *PIK3CA*; this mutation has been found in association with overgrowth syndromes and cancer growth.

Corresponding Author: Joyce Bischoff, Ph.D., Vascular Biology Program and Department of Surgery, Boston Children's Hospital, Harvard Medical School, Boston, MA 02115, Tel 617-919-2192, Fax 617-730-0231.

²Present address: Cancer and Blood Diseases Institute, Cincinnati Children's Hospital Medical Center, Cincinnati, OH, USA

The authors have declared that no conflict of interest exists.

Boscolo E.: AKT hyperphosphorylation in Lymphatic Malformation.

AUTHOR CONTRIBUTIONS

E.B., J.B. and M.L.W. designed the research. E.B. and S.C. performed the in vitro experiments, V.L.L. performed targeted sequencing. A.G., M.K. and M.L.W. assisted with data analysis and review of the manuscript. E.B. and J.B. wrote the manuscript.

ETHICAL STANDARDS

The experiments in this manuscript comply with the current laws of the United States of America.

CONFLICT OF INTEREST

The authors declare that they have no conflicts of interest.

LM-LEC exhibited angiogenic properties: both cellular proliferation and sprouting in collagen were significantly increased compared to HD-LEC. AKT-Thr308 was constitutively hyperphosphorylated in LM-LEC. Treatment of LM-LEC with PI3-Kinase inhibitors Wortmannin and LY294 decreased cellular proliferation and prevented the phosphorylation of AKT-Thr308 in both HD-LEC and LM-LEC. Treatment with the mTOR inhibitor rapamycin also diminished cellular proliferation, sprouting and AKT phosphorylation, but only in LM-LEC. Our results implicate disrupted PI3K-AKT signaling in LEC isolated from a human lymphatic malformation lesion.

Keywords

vascular anomaly; lymphatic vessels; PI3K; rapamycin; AKT

INTRODUCTION

The lymphatic system plays an essential role in fluid homeostasis, fat absorption and immune surveillance. During development lymphatic vessels originate from a subset of Prox1+ endothelial cells located on the dorsal side of the cardinal vein, around mouse embryonic day E9.5 (1–3). The Prox1+ endothelial cells form primary lymph sacs, and from these structures lymphatic vessels subsequently sprout in a process known as lymphangiogenesis.

Lymphatic malformations (LMs), also called lymphangioma or cystic hygroma, are composed of malformed, low-flow lymphatic channels (4–7). LMs are regarded as a developmental defect because of their early onset; they are evident at birth or become evident in early childhood (8). LMs tend to expand during adolescence and the lesions can affect vital organs, destroy bones, contribute to infections and cause disfigurement. The most common treatments are sclerotherapy for macrocystic (deep) LMs and surgical resection for microcystic (superficial) LMs. Lesions often recur after treatment (9–11).

LMs occur sporadically suggesting somatic mutations may be involved, but to date no causative mutation has been reported (12). Class I phosphoinositide 3-kinases (PI3Ks) are critical regulators of cell proliferation that act upon stimulation of upstream receptors by a growth factor or hormone. Class I PI3Ks are heterodimeric molecules composed of a catalytic subunit (p110 α , β , γ and δ) combined with a regulatory subunit (p85 α , p55 α , p50 α , p85 β and p55 γ) (13). Upon stimulation PI3Ks convert phosphatidylinositol-4,5-bisphosphate (PIP₂) to phosphatidylinositol-3,4,5-triphosphate (PIP₃) (14) leading to activation of the PH-domain containing serine-threonine kinase known as AKT. AKT phosphorylation is induced by PIP₃-dependent kinase 1 (PDK1) and is responsible for a variety of cellular activities such as cell proliferation, survival, and cell cycle entry (15). *PIK3CA*, encoding the PI3K catalytic subunit p110 α , is one of the most frequently mutated genes in human cancer (16, 17). Dominant activating mutations of *PIK3CA* have been identified in glioblastoma, breast, lung, and colon cancer (16, 18). The most frequent *PIK3CA* mutations reported are H1047R, E542K and E545K, and all of them stimulate kinase activity and exert oncogenic activity (19). A somatic activating *PIK3CA* mutation, H1047L, was also identified in congenital lipomatous overgrowth, vascular malformations, epidermal nevis, spinal/skeletal anomalies/

scoliosis (CLOVES) syndrome, a rare congenital disorder characterized by tissue overgrowth in extremities, vascular malformations and skin abnormalities (20). *PIK3CA* mutations were also detected in infiltrating lipomatosis (21) and in megalencephaly-capillary malformation (MCAP) syndrome (22).

Mutations in the PI3K regulatory subunit genes are also found in tumor samples. *PIK3R1* (p85 α) mutations were detected in glioblastoma, colorectal, breast and pancreatic tumor samples. Mutations in *PIK3R2* (p85 β) and *PIK3R3* (p55 γ) are rare (23). *PIK3R1* and *PIK3R2* have also been implicated in lymphatic development in mice and dysregulated overgrowth in humans, respectively (22, 24). *PIK3R3* function is not well understood, although it is thought to contribute to the growth of highly aggressive glioblastomas by mediating IGF2 receptor signaling to PI3K (25).

Here we show the angiogenic phenotype of lymphatic endothelial cells isolated from a patient-derived microcystic lymphatic malformation lesion (LM-LEC). We identified 2 mutations in these LM-LECs - a somatic mutation in the PI3K catalytic subunit *PIK3CA* and a germline mutation in the regulatory subunit *PIK3R3*. LM-LECs exhibited increased cell proliferation and AKT activation compared to human dermal lymphatic endothelial cells (HD-LEC). The PI3K inhibitors LY294 and Wortmannin inhibited cell proliferation and AKT activation in both HD- and LM-LEC, and prevented sprouting from LM-LEC derived spheroids. Of note, the mTOR inhibitor rapamycin decreased LM-LEC proliferation, sprouting, and activation of AKT, while no effect was noted on HD-LEC.

RESULTS

Isolation and characterization of lymphatic malformation endothelial cells (LM-LEC)

LM-LECs were isolated from surgically resected microcystic LM tissue by sequential anti-CD31 immuno-magnetic beads and anti-Podoplanin antibody selection. CD31+/Podoplanin + LM-LECs displayed cobblestone morphology typical of endothelial cells although the size of the LM-LECs appeared smaller than the control human dermal lymphatic endothelial cells (HD-LEC) (Fig.1A). Blood and lymphatic endothelial markers were assessed in LM-LECs, in comparison to HD-LECs, human umbilical vein endothelial cells (HUVEC) and cord blood derived endothelial colony forming cells (cbECFC) (Fig.1B). LM-LEC monolayers stained for blood and lymphatic endothelial markers CD31, VE-Cadherin and COUPTFII, and for lymphatic endothelial markers Podoplanin, PROX1 and LYVE1, and were negative for the fibroblast and smooth muscle markers CD90 and α -smooth muscle actin (α -SMA), respectively. Expression of COUP-TFII, Podoplanin, PROX1 and LYVE1 mRNA was confirmed by real-time qPCR in both LM-LEC and HD-LEC, with HUVECs shown for comparison (Fig.1C).

Germline and somatic *PIK3* mutations in LM-LEC

Targeted sequencing of a set of ten genes in the PI3K pathway (*AKT1*, *AKT2*, *AKT3*, *PIK3CA*, *PIK3CB*, *PIK3CG*, *PIK3R1*, *PIK3R2*, *PIK3R3*, *PTEN*) was performed in the LM-LECs (CD31+/Podoplanin+ LM cells) and returned 169,290 unique reads. Of these, 72,205 reads (49%) aligned to the genes included in the capture. The sample had >100X coverage

across 67% of the bases captured. In LM-LECs two mutations were identified in two different genes of the PI3K pathway: c.2140A>T (p.His1047Leu, H1047L) mutation in the *PIK3CA* gene and c.925C>T (p.Arg309STOP, R309STOP) mutation in the *PIK3R3* gene. The mutation in *PIK3CA* was seen in 9 out of 19 reads (47% variant) and the mutation in *PIK3R3* was seen in 126 out of 248 reads (51% variant). LM-LECs and CD31- cells isolated from the same LM patient were then tested for these two mutations by Sanger sequencing. Both the *PIK3CA* and the *PIK3R3* mutations were seen in the LM-LEC. In contrast, in the LM non-endothelial CD31- cells only the *PIK3R3* mutation was seen, confirming that the *PIK3CA* mutation was somatic whereas the *PIK3R3* mutation was inherited (Fig.2A). In both cell types, the *PIK3R3* mutation appeared to be heterozygous. *PIK3CA* mutation in LM-LEC appeared to be heterozygous as well.

DNA samples were obtained from the mother, father, and sibling of the patient. Sanger sequencing for both mutations showed that only the affected family member had the *PIK3CA* mutation but both the mother and the sibling had the heterozygous change in *PIK3R3* (Fig.2B), suggesting that the *PIK3CA* mutation was somatic whereas the *PIK3R3* mutation was inherited.

To confirm that both mutations were present in the patient tissue and were not a result of an advantageous mutation that arose during cell culture, DNA was extracted from LM tissue that had been frozen immediately after surgical removal. Sanger sequencing confirmed the presence of both *PIK3CA* and *PIK3R3* mutations. Furthermore, DNA subcloning and subsequent colony digestion with specific restriction enzymes showed the *PIK3R3* mutation with an allelic frequency of 31/48 (65%) (the mutation creates a site for the restriction enzyme BspCNI) and the *PIK3CA* mutation with an allelic frequency 2/48 (4%) (the mutation removes a site for BsaBI) (Fig.2C). The lower frequency of *PIK3CA* mutation in the DNA from the frozen tissue is not surprising as no sorting was performed and the relative abundance of endothelial cells is much lower compared to non-endothelial cell types that do not contain the mutation.

Pro-angiogenic properties of LM-LEC

Next we analyzed the angiogenic properties of LM-LEC vs. HD-LEC. LM-LECs proliferated faster than HD-LEC when cultured either in growth (EGM2/20%FBS), starvation (EBM2/no growth factors/10%FBS), and serum-free (EBM2/no growth factors/no FBS) media (Fig.3A). HD-LECs sprouted only in the presence of 250ng/ml of VEGF-C, when re-suspended in 3-dimensional collagen gels as spheroids (Fig.3B). In contrast, LM-LEC extended tubular structures in the presence or absence of the lymphangiogenic factor VEGF-C.

We next analyzed the activation status of AKT, a critical downstream target of PI3K and mediator of angiogenic signals. LM-LEC showed strong upregulation (2.7 fold) of phospho-AKT-Thr308 (P-AKT) compared to HD-LEC (Fig.3C), while levels of the MAP kinase phospho-ERK (P-ERK) were similar. Furthermore, real-time qPCR analysis of the lymphangiogenesis factors VEGF-C and VEGF-D in LM-LEC revealed a 1.5 and 2 fold upregulation of gene expression compared to HD-LEC (Fig.3D). VEGFR-3 and Neuropilin-2 (NRP2) mRNA levels in LM-LEC were higher than HD-LEC, and VEGFR-3

and NRP2 protein expression in LM-LEC were 2.6 and 11.7 times higher than HD-LEC, respectively (Fig.3E). Thus, these results demonstrate that LM-LECs exhibited increased AKT activation and increased expression of lymphangiogenesis factors and receptors, which could explain the enhanced pro-angiogenic activities compared to HD-LEC.

PI3K inhibitors and rapamycin prevent the pro-angiogenic phenotype of LM-LEC

To determine whether inhibition of PI3K pathway would inhibit the pro-angiogenic activities of LM-LEC, we assessed the effects of the PI3K inhibitors LY294 and Wortmannin on LM-LEC proliferation, spheroid sprouting and AKT phosphorylation (Fig. 4). We also assessed the effect of the mTOR inhibitor rapamycin since it has been reported that rapamycin suppresses lymphangiogenesis and lymphatic metastasis in mice and zebrafish (26–29). LM-LEC proliferation was significantly ($p<0.05$) decreased in response to 48h treatment with rapamycin, LY294, and Wortmannin 10 μ M (Fig.4A). In contrast, HD-LEC proliferation was affected by LY294 and Wortmannin 10 μ M treatment, but not by rapamycin. In a second angiogenesis assay, LM-LEC formed sprouts from spheroids in collagen gels. Each drug caused a significant ($p<0.05$) reduction of LM-LEC spheroid sprout number. At the highest concentration tested, rapamycin reduced the number of sprouts by 30.5%, LY294 by 78.1%, and Wortmannin by 94.5% (Fig.4B).

Phosphorylation of AKT-Thr308 was significantly lower after LM-LECs treatment for 48 hours with rapamycin, LY294 and Wortmannin (Fig.4C). Conversely, in HD-LEC, the levels of phospho-AKT-Thr308 were affected by the PI3K inhibitors LY294 and Wortmannin, but not by rapamycin. Of interest, in response to LY294, phospho-ERK expression increased in both LM- and HD- LEC; this increased ERK activation was previously shown in HUVECs with RAF1S^{259A}-induced impaired AKT signaling (30, 31).

DISCUSSION

Here we identify two mutations in PI3K pathway genes in LEC from a lymphatic malformation lesion (LM-LEC). Our analyses of the pro-angiogenic properties and the response to specific inhibitors of the patient-derived LM-LEC suggest a role for *PIK3* mutations and AKT hyper-activation in lymphatic malformation development. Inhibitors of PI3K and mTOR pathways can diminish AKT phosphorylation and suppress cell proliferation and sprouting in LM-LECs carrying *PIK3* mutations.

Lymphatic malformations (LM) are vascular lesions composed of dilated lymphatic channels often disconnected from the normal lymphatic system (32). Lymphatic vessels develop in the embryo from a subset of Prox1+ endothelial cells that, in response to VEGF-C, form lymph sacs that transiently fill with blood until separation from the cardinal vein and formation of lymphovenous valves (2, 3, 33, 34). LMs are a result of a congenital/early defect in the development of the lymphatic system, possibly caused by incomplete maturation of the Prox1+ endothelial cells or migration of a small subpopulation of the Prox1+ cells to the incorrect site. In LMs, dilated channels are filled with lymphatic and blood fluids (35), suggesting there could be an incomplete separation from the blood circulation.

Recently, Turner and colleagues proposed that integrin $\alpha 5\beta 1$ in Prox1+/Pdgfrb+ LEC is required for lymphovenous valve formation, enabling correct lymphatic-blood vessel separation. In fact *Itga5^{Pdgfrb-cre}* mice embryos show blood-filled hyperplastic lymphatic vessels, reminiscent of LMs. Integrin $\alpha 5\beta 1$ is required for VEGFR-3 activation (36), therefore disruption of the VEGFR-3 signaling is likely to be responsible for defects in the formation of the lymphatic system. VEGFR-3 cooperates with NRP2 to promote lymphatic vessel development and sprouting (37, 38). In our study we show that LM-LEC overexpress NRP2 and VEGFR-3 and the VEGFR-3 ligands VEGF-C and VEGF-D. These findings suggest that LM-LECs have a pro-lymphangiogenic phenotype; similarly VEGFR-3/NRP2 overexpression has been described in a subset of vascular malformation ECs (39). VEGFR-3 signaling can activate the PI3K/AKT pathway (40) and this signaling cascade has been shown to be critical for lymphatic development in mice (41) and for LEC migration in vitro (42). Whether and to what extent VEGFR-3 and NRP-2 interact with the mutant *PIK3R3* and *PIK3CA* polypeptide products was not addressed in this study.

Germline mutations in *VEGFR3* and in genes of the VEGFR-3 signaling pathway are involved in familial lymphatic abnormalities such as primary lymphedema, a defect of lymphatic drainage (for which mutations in *VEGF-C*, *VEGFR3*, *FOXC2*, *SOX18*, *CCBE1*, *PTPN14*, and *NEMO* have been identified) (43–47). These were not among the 10 PI3K pathway genes that were sequenced in this study, therefore, we cannot rule in or rule out mutations in these genes in the LM-LECs.

LMs are non-familial sporadic lesions, therefore it has been postulated (32) that somatic mutations restricted to the cells in the affected area are the cause for LM. In the LM tissue from one patient, we detected mutations in *PIK3R3* and *PIK3CA*, two genes that are part of the PI3K signaling pathway. The *PIK3R3* mutation is a germline mutation as it was also detected in the mother and sibling and it is present in all of the cells of the LM patient. The *PIK3CA* mutation is a somatic mutation: it was detected at low allelic frequency in the LM tissue, but at ~50% in the LM-LEC, indicating likely heterozygosity. Concurrent with our study, *PIK3CA* somatic mutations have been identified in a subset of vascular anomalies associated with/comprised of a lymphatic malformation (48).

The *PIK3R3* germline mutation detected in the LM patient is a p.R309stop, which would cause premature truncation of the polypeptide and potentially non-sense mediated decay of the mRNA. Therefore, the p.R309stop may be a loss of function mutation. To date there is no report of a *PIK3R3* knock-out mouse model, and thus the role of *PIK3R3* during development remains elusive. It is possible that, in subjects with only the germline *PIK3R3* mutation, genes encoding for other PI3K regulatory subunits (*PIK3R1* and *PIK3R2*) could compensate for the loss of PI3KR3 function and thus, another mutation in the PI3K pathway is required for LM to develop. Indeed, it has been shown that *Pik3r1* is essential for embryonic lymphangiogenesis, and its targeted deletion impairs lymphatic sprouting and maturation in the gut and diaphragm (24).

PIK3CA encodes for the p110 α catalytic subunit and is expressed ubiquitously in cells throughout the body. *PIK3CA* somatic mutations, detected in a wide array of cancers (16, 17), have also been found in association with overgrowth syndromes with a lymphatic or

vascular malformation component, such as CLOVES (Congenital Lipomatous asymmetric Overgrowth of the trunk, lymphatic, capillary, venous, and combined-type Vascular malformations, Epidermal nevi, Skeletal and spinal anomalies) (20), MCAP (Megaencephaly-Capillary Malformation syndrome) and FH (Fibroadipose Hyperplasia), respectively (49). Mutations in some of the PI3K-AKT pathway genes that we sequenced in the LM-LECs, such as *PTEN*, *AKT1*, *AKT2*, and *AKT3*, have been implicated in other overgrowth syndromes (50–52).

Although LMs are considered a vascular malformation, some investigators regard LMs as a benign neoplasm (53) since LM-LEC have high proliferative potential and can form LM-like lesions when injected into mice (54). The LM-LEC isolated herein, with the *PIK3CA* p.H1047L and *PIK3R3* p.R309stop mutations, exhibit high cellular proliferative and sprouting potential, as well as increased AKT phosphorylation. The PI3K inhibitors Wortmannin and LY294 impaired cellular proliferation and sprouting, and prevented AKT phosphorylation in LM-LECs. These inhibitors also strongly reduced cellular proliferation and AKT activation in normal HD-LEC. Interestingly, strong phospho-AKT inhibition, caused by LY294, increased phospho-ERK levels in both HD-LEC and LM-LEC. Signaling through the ERK pathway was recently shown to be essential for LEC fate specification (55), when phospho-AKT is ablated, ERK signaling is increased, inducing Sox18 and Prox1 expression and subsequent lymphangectasia. This suggests that excessive ERK signaling can also be detrimental for the lymphatic system development.

PI3K inhibitors are currently being tested in clinical trials, however only the p110 δ -selective inhibitor (GS-1101/Idelalisib) has been approved by the FDA for treatment of relapsed chronic lymphocytic leukemia (CLL) (56). The mTOR inhibitor rapamycin, compared to the PI3K inhibitors we tested, had a milder effect on reducing AKT phosphorylation, proliferation and sprouting of LM-LEC, but interestingly, in this study, it had no effect on normal HD-LEC. Rapamycin was shown to prevent lymphangiogenesis in a head and neck squamous carcinoma murine model and during wound healing (27–29). In fact, one of the targets of rapamycin in LEC is VEGFR-3 expression (57). A retrospective evaluation of rapamycin effects in 6 patients with life-threatening vascular anomalies showed it is effective and safe (58). Furthermore, a clinical trial for the rapamycin treatment of complicated vascular anomalies, including microcystic lymphatic malformations, is ongoing (NCT00975819).

In summary, we demonstrate that mutations in *PIK3* can be associated with LMs, and that pharmacological therapies targeting the increased AKT phosphorylation observed in LEC isolated from LM lesions may be considered, alone or in combination, for the treatment of LMs. Further studies are needed to determine if our results from 1 LM sample can be generalized to other LM tissues with the *PIK3CA* mutation we identified or other *PIK3CA* activating mutations. In addition, the contribution of the *PIK3R3* mutation to the LM phenotype needs to be considered for future investigations.

MATERIALS AND METHODS

Cell Isolation and Culture

Specimens of LM were obtained under a human subject protocol approved by the Committee on Clinical Investigation, Boston Children's Hospital. The clinical diagnosis was confirmed in the Department of Pathology at Boston Children's Hospital. Informed consent was obtained for the specimens, according to the Declaration of Helsinki. Single cell suspensions were prepared from the LM specimens by digesting with collagenase (Roche). Cells were seeded on fibronectin-coated tissue culture dishes in EGM2/20% fetal bovine serum (FBS) (Lonza). When the cells reached 80% confluency, they were purified with anti-CD31 conjugated magnetic beads (Dyna). When the CD31-positive cells were again subconfluent, they were reselected with anti-podoplanin antibody (Covance) followed by magnetic beads conjugated with anti-mouse IgG. Cells were analyzed for lymphatic endothelial cell markers and named lymphatic malformation-lymphatic endothelial cells (LM-LEC). LM-LEC at passage 6 were analyzed for karyotype and found to be normal 46, X,Y. Normal human dermal lymphatic endothelial cells (HD-LEC) were purchased from Lonza. Human umbilical cord endothelial colony forming cells (ECFC) were isolated as previously described (59, 60). HUVECs were a kind gift from Dr. Tanya Mayadas, Vascular Research Division, Brigham and Women's Hospital. HD-LEC, ECFCs and HUVECs were cultured in the same conditions as LM-LECs.

qRT-PCR

Total RNA was extracted using the RNeasy kit (Qiagen). cDNA was prepared using Superscript II enzyme (Invitrogen Corp.) and 2 µg total RNA. For real-time qPCR analysis, the DyNAmo Sybr-Green-based system (New England BioLabs) was used. Oligonucleotide primers are listed in Supplementary Table S1. Reactions were run on a LightCycler (Roche Applied Science). Each experiment was done in triplicate and repeated two times.

DNA preparation for target capture

DNA was extracted from the cultured LM-LECs and from frozen tissue using the QIAamp DNA Mini Kit (Qiagen). A genomic library was prepared from the LEC DNA as previously described (20). Briefly, 3µg of DNA was mechanically sheared into 100–200 basepair (bp) fragments. A unique 4 bp barcode was added to the ends of the DNA fragments. Following 16 cycles of PCR, the DNA was hybridized for 65 hours to a custom designed capture array (Agilent Technology 1M SureSelect DNA Capture Array). The array contained the coding regions of 10 genes within the PI3K signaling pathway (*AKT1*, *AKT2*, *AKT3*, *PIK3CA*, *PIK3CB*, *PIK3CG*, *PIK3R1*, *PIK3R2*, *PIK3R3*, *PTEN*). Post-capture, another 17 cycles of PCR were performed. The samples were then sequenced by 100-bp paired end sequencing on an Illumina HiSeq2 sequencer (Illumina, Inc.).

DNA Sequence Analysis

Paired-end reads from the Illumina HiSeq2 were de-barcoded with Novobarcode (Novocraft Technologies) and aligned to the UCSC Human reference genome (GRCh37) using the Burrows-Wheeler Aligner (version 0.6.1). Pileup files were generated using SAMtools.

Variants found in the 1000 Genomes database, the NHLBI Exome Variant Server, or the Database of Common SNPs (dbSNP, build 132) were filtered out.

Mutation Confirmation

Mutations were confirmed with Sanger sequencing and restriction enzyme digest. Sanger sequencing was performed by PCR amplification of the DNA around the mutation. In addition, both mutations changed the cut sites of unique enzymes. The *PIK3CA* p.H1047L base change removes a restriction site for BsaBI. The *PIK3R3* base change creates a restriction site for BspCNI. DNA fragments were amplified by PCR then inserted into a plasmid vector using the TOPO TA Cloning Kit (Life Technologies). One Shot TOP-10 chemically competent *E.coli* were transformed and colonies cultured. Enzyme digests were performed with DNA from individual colonies.

Immunocytochemistry

LM-LECs, HD-LECs, HUVECs and cbECFCs were cultured until subconfluent, fixed with cold methanol and stained with anti- CD31 (1:100, Dako), VE-Cadherin (1:100, Santa Cruz), COUPTFII (1:100, R&D Systems), Podoplanin (1:100, Covance), Prox1 (1:100, Angiobio), LYVE1 (1:100, Abcam), CD90 (1:100, BD Biosciences), and α SMA (1:1000, Sigma). Cells were then incubated with FITC-labeled secondary antibody (1:200, Vector Laboratories) and nuclei counterstained with DAPI (Vector Laboratories).

Microscope Image acquisition

Fluorescence images were taken with Leica TCS SP2 Acousto-Optical Beam Splitter confocal system equipped with DMIRE2 inverted microscope (Diode 405 nm, Argon 488 nm, HeNe 594 nm; Leica Microsystems), Leica Confocal Software Version 2.61, Build 1537. Images were taken at room temperature (about 20 C) and files always exported as 8 bit format.

Assays for In Vitro Cellular Proliferation

LEC proliferation was assessed after seeding the cells at 10^4 cell/cm² on 48-well plates. Following attachment (24 h), plating efficiency was determined, and cell number was determined after 24, 48, 72, and 96hs, using a Coulter Counter® (Beckman) or by manual cell counting with hemocytometer.

Spheroid-based lymphangiogenesis assay

Early passage LM-LECs and HD-LECs were suspended and aggregated overnight to form cellular spheroids (500 cells/spheroid). LEC spheroids were embedded into collagen gels and either left untreated or treated for 16h with 250 ng/ml VEGF-C. Inhibitors were mixed with the collagen gel before polymerization and images were taken after 16 hours. *In vitro* angiogenesis was quantified by measuring the number of sprouts grown out of each spheroid using NIH ImageJ software. Ten to fifteen spheroids per experimental group were analyzed.

Immunoblot

Cells were lysed with RIPA buffer (Boston Bioproducts), containing a phosphatase inhibitor cocktail (Roche). Lysates were subjected to SDS-PAGE and transferred to Immobilon-P membrane. Membranes were incubated with antibodies against the following: VEGFR-3 (1:1000, BD Bioscience), NRP2 and VE-Cadherin (both 1:500 Santa Cruz Biotech), phospho-AKT (Thr308), AKT, phospho-ERK, ERK (all in 1:1000, Cell Signaling Technology), Tubulin (1:5000, Sigma-Aldrich). Membranes were incubated with peroxidase-conjugated secondary antibodies (1:5000, Vector Laboratories). Antigen-antibody complexes were visualized using ECL and chemiluminescent sensitive film (Pierce). Band intensity was analyzed with ImageJ software.

Inhibitors

The inhibitors used in this study were rapamycin at 1 and 10nM (LC Laboratories), LY294 at 50 and 100 μ M and Wortmannin at 1 and 10 μ M (Sigma Aldrich).

Statistical Analysis

The data were expressed as means \pm s.d.m. or means \pm s.e.m. and analyzed by ANOVA followed by Student's t-test where appropriate. Differences were considered significant at p values < 0.05 .

Supplementary Material

Refer to Web version on PubMed Central for supplementary material.

Acknowledgments

Research reported in this manuscript was supported by a Translational Research Program Pilot Study Grant from Boston Children's Hospital (J.B.), the Charles Hood Foundation (E.B.), the Manton Center for Orphan Disease Research (E.B.), and the National Heart, Lung, and Blood Institute, part of the National Institutes of Health, under Award Number R01 HL117952 (E.B.). The content is solely the responsibility of the authors and does not necessarily represent the official views of the National Institutes of Health. We thank Dr. Steven Fishman, and Lan Huang for helpful discussions, Drs. Camille L. Stewart and Annie Kulungowski for initial characterization of the LM-LEC, Dr. Tanya Mayadas for providing HUVECs, the Cytogenetics Core of Dana Farber Harvard Cancer Center (P30 CA006516), Jill Wylie-Sears for technical assistance and Kristin Johnson for the preparation of figures.

Non-standard abbreviations

LM	lymphatic malformation
LEC	lymphatic endothelial cells
PI3K	phosphoinositide 3-kinase

BIBLIOGRAPHY

1. Wigle JT, Harvey N, Detmar M, Lagutina I, Grosveld G, Gunn MD, Jackson DG, Oliver G. An essential role for Prox1 in the induction of the lymphatic endothelial cell phenotype. *EMBO J*. 2002; 21(7):1505–13. [PubMed: 11927535]
2. Wigle JT, Oliver G. Prox1 function is required for the development of the murine lymphatic system. *Cell*. 1999; 98(6):769–78. [PubMed: 10499794]

3. Srinivasan RS, Dillard ME, Lagutin OV, Lin FJ, Tsai S, Tsai MJ, Samokhvalov IM, Oliver G. Lineage tracing demonstrates the venous origin of the mammalian lymphatic vasculature. *Genes Dev.* 2007; 21(19):2422–32. [PubMed: 17908929]
4. Mulliken JB, Glowacki J. Classification of pediatric vascular lesions. *Plast Reconstr Surg.* 1982; 70(1):120–1. [PubMed: 7089103]
5. Padwa BL, Hayward PG, Ferraro NF, Mulliken JB. Cervicofacial lymphatic malformation: clinical course, surgical intervention, and pathogenesis of skeletal hypertrophy. *Plast Reconstr Surg.* 1995; 95(6):951–60. [PubMed: 7732142]
6. Whimster IW. The pathology of lymphangioma circumscriptum. *Br J Dermatol.* 1976; 94(5):473–86. [PubMed: 1268059]
7. Brouillard P, Vikkula M. Vascular malformations: localized defects in vascular morphogenesis. *Clinical genetics.* 2003; 63(5):340–51. [PubMed: 12752563]
8. Garzon MC, Huang JT, Enjolras O, Frieden IJ. Vascular malformations - Part I. *J Am Acad Dermatol.* 2007; 56(3):353–70. [PubMed: 17317485]
9. Fageeh N, Manoukian J, Tewfik T, Schloss M, Williams HB, Gaskin D. Management of head and neck lymphatic malformations in children. *J Otolaryngol.* 1997; 26(4):253–8. [PubMed: 9263895]
10. Hancock BJ, Stvil D, Luks FI, Dilorenzo M, Blanchard H. Complications of Lymphangiomas in Children. *J Pediatr Surg.* 1992; 27(2):220–6. [PubMed: 1564622]
11. Jackson IT, Carreno R, Potparic Z, Hussain K. Hemangiomas, Vascular Malformations, and Lymphovenous Malformations - Classification and Methods of Treatment. *Plast Reconstr Surg.* 1993; 91(7):1216–30. [PubMed: 8497521]
12. Uebelhoer M, Boon LM, Vikkula M. Vascular Anomalies: From Genetics toward Models for Therapeutic Trials. *Csh Perspect Med.* 2012; 2(8)
13. Fruman DA, Meyers RE, Cantley LC. Phosphoinositide kinases. *Annual review of biochemistry.* 1998; 67:481–507.
14. Whitman M, Downes CP, Keeler M, Keller T, Cantley L. Type I phosphatidylinositol kinase makes a novel inositol phospholipid, phosphatidylinositol-3-phosphate. *Nature.* 1988; 332(6165):644–6. [PubMed: 2833705]
15. Lawlor MA, Alessi DR. PKB/Akt: a key mediator of cell proliferation, survival and insulin responses? *Journal of cell science.* 2001; 114(Pt 16):2903–10. [PubMed: 11686294]
16. Samuels Y, Wang Z, Bardelli A, Silliman N, Ptak J, Szabo S, Yan H, Gazdar A, Powell SM, Riggins GJ, et al. High frequency of mutations of the PIK3CA gene in human cancers. *Science.* 2004; 304(5670):554. [PubMed: 15016963]
17. Samuels Y, Ericson K. Oncogenic PI3K and its role in cancer. *Current opinion in oncology.* 2006; 18(1):77–82. [PubMed: 16357568]
18. Wood LD, Parsons DW, Jones S, Lin J, Sjoblom T, Leary RJ, Shen D, Boca SM, Barber T, Ptak J, et al. The genomic landscapes of human breast and colorectal cancers. *Science.* 2007; 318(5853):1108–13. [PubMed: 17932254]
19. Bader AG, Kang S, Vogt PK. Cancer-specific mutations in PIK3CA are oncogenic in vivo. *Proc Natl Acad Sci U S A.* 2006; 103(5):1475–9. [PubMed: 16432179]
20. Kurek KC, Luks VL, Ayturk UM, Alomari AI, Fishman SJ, Spencer SA, Mulliken JB, Bowen ME, Yamamoto GL, Kozakewich HP, et al. Somatic mosaic activating mutations in PIK3CA cause CLOVES syndrome. *Am J Hum Genet.* 2012; 90(6):1108–15. [PubMed: 22658544]
21. Maclellan RA, Luks VL, Vivero MP, Mulliken JB, Zurakowski D, Padwa BL, Warman ML, Greene AK, Kurek KC. PIK3CA activating mutations in facial infiltrating lipomatosis. *Plast Reconstr Surg.* 2014; 133(1):12e–9e.
22. Riviere JB, Mirzaa GM, O'Roak BJ, Beddaoui M, Alcantara D, Conway RL, St-Onge J, Schwartzenuber JA, Gripp KW, Nikkel SM, et al. De novo germline and postzygotic mutations in AKT3, PIK3R2 and PIK3CA cause a spectrum of related megalencephaly syndromes. *Nat Genet.* 2012; 44(8):934–40. [PubMed: 22729224]
23. Kandoth C, McLellan MD, Vandin F, Ye K, Niu B, Lu C, Xie M, Zhang Q, McMichael JF, Wyczalkowski MA, et al. Mutational landscape and significance across 12 major cancer types. *Nature.* 2013; 502(7471):333–9. [PubMed: 24132290]

24. Mouta-Bellum C, Kirov A, Miceli-Libby L, Mancini ML, Petrova TV, Liaw L, Prudovsky I, Thorpe PE, Miura N, Cantley LC, et al. Organ-specific lymphangiectasia, arrested lymphatic sprouting, and maturation defects resulting from gene-targeting of the PI3K regulatory isoforms p85alpha, p55alpha, and p50alpha. *Developmental dynamics : an official publication of the American Association of Anatomists*. 2009; 238(10):2670–9. [PubMed: 19705443]
25. Soroceanu L, Kharbanda S, Chen R, Soriano RH, Aldape K, Misra A, Zha J, Forrest WF, Nigro JM, Modrusan Z, et al. Identification of IGF2 signaling through phosphoinositide-3-kinase regulatory subunit 3 as a growth-promoting axis in glioblastoma. *Proc Natl Acad Sci U S A*. 2007; 104(9):3466–71. [PubMed: 17360667]
26. Flores MV, Hall CJ, Crosier KE, Crosier PS. Visualization of embryonic lymphangiogenesis advances the use of the zebrafish model for research in cancer and lymphatic pathologies. *Developmental dynamics : an official publication of the American Association of Anatomists*. 2010; 239(7):2128–35. [PubMed: 20549745]
27. Huber S, Bruns CJ, Schmid G, Hermann PC, Conrad C, Niess H, Huss R, Graeb C, Jauch KW, Heeschen C, et al. Inhibition of the mammalian target of rapamycin impedes lymphangiogenesis. *Kidney international*. 2007; 71(8):771–7. [PubMed: 17299523]
28. Kobayashi S, Kishimoto T, Kamata S, Otsuka M, Miyazaki M, Ishikura H. Rapamycin, a specific inhibitor of the mammalian target of rapamycin, suppresses lymphangiogenesis and lymphatic metastasis. *Cancer science*. 2007; 98(5):726–33. [PubMed: 17425689]
29. Patel V, Marsh CA, Dorsam RT, Mikelis CM, Masedunskas A, Amornphimoltham P, Nathan CA, Singh B, Weigert R, Molinolo AA, et al. Decreased lymphangiogenesis and lymph node metastasis by mTOR inhibition in head and neck cancer. *Cancer Res*. 2011; 71(22):7103–12. [PubMed: 21975930]
30. Deng Y, Atri D, Eichmann A, Simons M. Endothelial ERK signaling controls lymphatic fate specification. *J Clin Invest*. 2013; 123(3):1202–15. [PubMed: 23391722]
31. Ren B, Deng Y, Mukhopadhyay A, Lanahan AA, Zhuang ZW, Moodie KL, Mulligan-Kehoe MJ, Byzova TV, Peterson RT, Simons M. ERK1/2-Akt1 crosstalk regulates arteriogenesis in mice and zebrafish. *J Clin Invest*. 2010; 120(4):1217–28. [PubMed: 20237411]
32. Brouillard P, Boon L, Vikkula M. Genetics of lymphatic anomalies. *J Clin Invest*. 2014; 124(3):898–904. [PubMed: 24590274]
33. Francois M, Short K, Secker GA, Combes A, Schwarz Q, Davidson TL, Smyth I, Hong YK, Harvey NL, Koopman P. Segmental territories along the cardinal veins generate lymph sacs via a ballooning mechanism during embryonic lymphangiogenesis in mice. *Dev Biol*. 2012; 364(2):89–98. [PubMed: 22230615]
34. Hagerling R, Pollmann C, Andreas M, Schmidt C, Nurmi H, Adams RH, Alitalo K, Andresen V, Schulte-Merker S, Kiefer F. A novel multistep mechanism for initial lymphangiogenesis in mouse embryos based on ultramicroscopy. *EMBO J*. 2013; 32(5):629–44. [PubMed: 23299940]
35. Elluru RG, Balakrishnan K, Padua HM. Lymphatic malformations: Diagnosis and management. *Seminars in pediatric surgery*. 2014; 23(4):178–85. [PubMed: 25241095]
36. Zhang X, Groopman JE, Wang JF. Extracellular matrix regulates endothelial functions through interaction of VEGFR-3 and integrin alpha5beta1. *Journal of cellular physiology*. 2005; 202(1):205–14. [PubMed: 15389531]
37. Xu Y, Yuan L, Mak J, Pardanaud L, Caunt M, Kasman I, Larrivee B, Del Toro R, Suchting S, Medvinsky A, et al. Neuropilin-2 mediates VEGF-C-induced lymphatic sprouting together with VEGFR3. *J Cell Biol*. 2010; 188(1):115–30. [PubMed: 20065093]
38. Yuan L, Moyon D, Pardanaud L, Breant C, Karkkainen MJ, Alitalo K, Eichmann A. Abnormal lymphatic vessel development in neuropilin 2 mutant mice. *Development*. 2002; 129(20):4797–806. [PubMed: 12361971]
39. Partanen TA, Vuola P, Jauhiainen S, Lohi J, Salminen P, Pitkaranta A, Hakkinen SK, Honkonen K, Alitalo K, Yla-Herttuala S. Neuropilin-2 and vascular endothelial growth factor receptor-3 are up-regulated in human vascular malformations. *Angiogenesis*. 2013; 16(1):137–46. [PubMed: 22961441]

40. Coso S, Zeng Y, Opeskin K, Williams ED. Vascular endothelial growth factor receptor-3 directly interacts with phosphatidylinositol 3-kinase to regulate lymphangiogenesis. *PLoS One*. 2012; 7(6):e39558. [PubMed: 22745786]
41. Zhou F, Chang Z, Zhang L, Hong YK, Shen B, Wang B, Zhang F, Lu G, Tvorogov D, Alitalo K, et al. Akt/Protein kinase B is required for lymphatic network formation, remodeling, and valve development. *Am J Pathol*. 2010; 177(4):2124–33. [PubMed: 20724596]
42. Makinen T, Veikkola T, Mustjoki S, Karpanen T, Catimel B, Nice EC, Wise L, Mercer A, Kowalski H, Kerjaschki D, et al. Isolated lymphatic endothelial cells transduce growth, survival and migratory signals via the VEGF-C/D receptor VEGFR-3. *EMBO J*. 2001; 20(17):4762–73. [PubMed: 11532940]
43. Gordon K, Schulte D, Brice G, Simpson MA, Roukens MG, van Impel A, Connell F, Kalidas K, Jeffery S, Mortimer PS, et al. Mutation in vascular endothelial growth factor-C, a ligand for vascular endothelial growth factor receptor-3, is associated with autosomal dominant milroy-like primary lymphedema. *Circ Res*. 2013; 112(6):956–60. [PubMed: 23410910]
44. Irrthum A, Karkkainen MJ, Devriendt K, Alitalo K, Vikkula M. Congenital hereditary lymphedema caused by a mutation that inactivates VEGFR3 tyrosine kinase. *Am J Hum Genet*. 2000; 67(2):295–301. [PubMed: 10856194]
45. Irrthum A, Devriendt K, Chitayat D, Matthijs G, Glade C, Steijlen PM, Fryns JP, Van Steensel MA, Vikkula M. Mutations in the transcription factor gene SOX18 underlie recessive and dominant forms of hypotrachosis-lymphedema-telangiectasia. *Am J Hum Genet*. 2003; 72(6):1470–8. [PubMed: 12740761]
46. Connell F, Kalidas K, Ostergaard P, Brice G, Homfray T, Roberts L, Bunyan DJ, Mitton S, Mansour S, Mortimer P, et al. Linkage and sequence analysis indicate that CCBE1 is mutated in recessively inherited generalised lymphatic dysplasia. *Human genetics*. 2010; 127(2):231–41. [PubMed: 19911200]
47. Au AC, Hernandez PA, Lieber E, Nadroo AM, Shen YM, Kelley KA, Gelb BD, Diaz GA. Protein tyrosine phosphatase PTPN14 is a regulator of lymphatic function and choanal development in humans. *Am J Hum Genet*. 2010; 87(3):436–44. [PubMed: 20826270]
48. Osborn AJ, Dickie P, Neilson DE, Glaser K, Lynch KA, Gupta A, Hsi Dickie B. Activating PIK3CA Alleles and Lymphangiogenic Phenotype of Lymphatic Endothelial Cells Isolated from Lymphatic Malformations. *Hum Mol Genet*. 2014 In press.
49. Lindhurst MJ, Parker VE, Payne F, Sapp JC, Rudge S, Harris J, Witkowski AM, Zhang Q, Groeneveld MP, Scott CE, et al. Mosaic overgrowth with fibroadipose hyperplasia is caused by somatic activating mutations in PIK3CA. *Nat Genet*. 2012; 44(8):928–33. [PubMed: 22729222]
50. Hussain K, Challis B, Rocha N, Payne F, Minic M, Thompson A, Daly A, Scott C, Harris J, Smillie BJ, et al. An activating mutation of AKT2 and human hypoglycemia. *Science*. 2011; 334(6055):474. [PubMed: 21979934]
51. Lindhurst MJ, Sapp JC, Teer JK, Johnston JJ, Finn EM, Peters K, Turner J, Cannons JL, Bick D, Blakemore L, et al. A mosaic activating mutation in AKT1 associated with the Proteus syndrome. *N Engl J Med*. 2011; 365(7):611–9. [PubMed: 21793738]
52. Poduri A, Evrony GD, Cai X, Elhosary PC, Beroukhi R, Lehtinen MK, Hills LB, Heinzen EL, Hill A, Hill RS, et al. Somatic activation of AKT3 causes hemispheric developmental brain malformations. *Neuron*. 2012; 74(1):41–8. [PubMed: 22500628]
53. Huang HY, Ho CC, Huang PH, Hsu SM. Co-expression of VEGF-C and its receptors, VEGFR-2 and VEGFR-3, in endothelial cells of lymphangioma. Implication in autocrine or paracrine regulation of lymphangioma. *Lab Invest*. 2001; 81(12):1729–34. [PubMed: 11742043]
54. Lokmic Z, Mitchell GM, Koh Wee Chong N, Bastiaanse J, Gerrand YW, Zeng Y, Williams ED, Penington AJ. Isolation of human lymphatic malformation endothelial cells, their in vitro characterization and in vivo survival in a mouse xenograft model. *Angiogenesis*. 2014; 17(1):1–15. [PubMed: 23884796]
55. Deng Y, Atri D, Eichmann A, Simons M. Endothelial ERK signaling controls lymphatic fate specification. *The Journal of clinical investigation*. 2013; 123(3):1202–15. [PubMed: 23391722]
56. Fruman DA, Rommel C. PI3K and cancer: lessons, challenges and opportunities. *Nature reviews Drug discovery*. 2014; 13(2):140–56.

57. Luo Y, Liu L, Rogers D, Su W, Odaka Y, Zhou H, Chen W, Shen T, Alexander JS, Huang S. Rapamycin inhibits lymphatic endothelial cell tube formation by downregulating vascular endothelial growth factor receptor 3 protein expression. *Neoplasia*. 2012; 14(3):228–37. [PubMed: 22496622]
58. Hammill AM, Wentzel M, Gupta A, Nelson S, Lucky A, Elluru R, Dasgupta R, Azizkhan RG, Adams DM. Sirolimus for the treatment of complicated vascular anomalies in children. *Pediatr Blood Cancer*. 2011; 57(6):1018–24. [PubMed: 21445948]
59. Ingram DA, Caplice NM, Yoder MC. Unresolved questions, changing definitions, and novel paradigms for defining endothelial progenitor cells. *Blood*. 2005; 106(5):1525–31. [PubMed: 15905185]
60. Melero-Martin JM, Khan ZA, Picard A, Wu X, Paruchuri S, Bischoff J. In vivo vasculogenic potential of human blood-derived endothelial progenitor cells. *Blood*. 2007; 109(11):4761–8. [PubMed: 17327403]

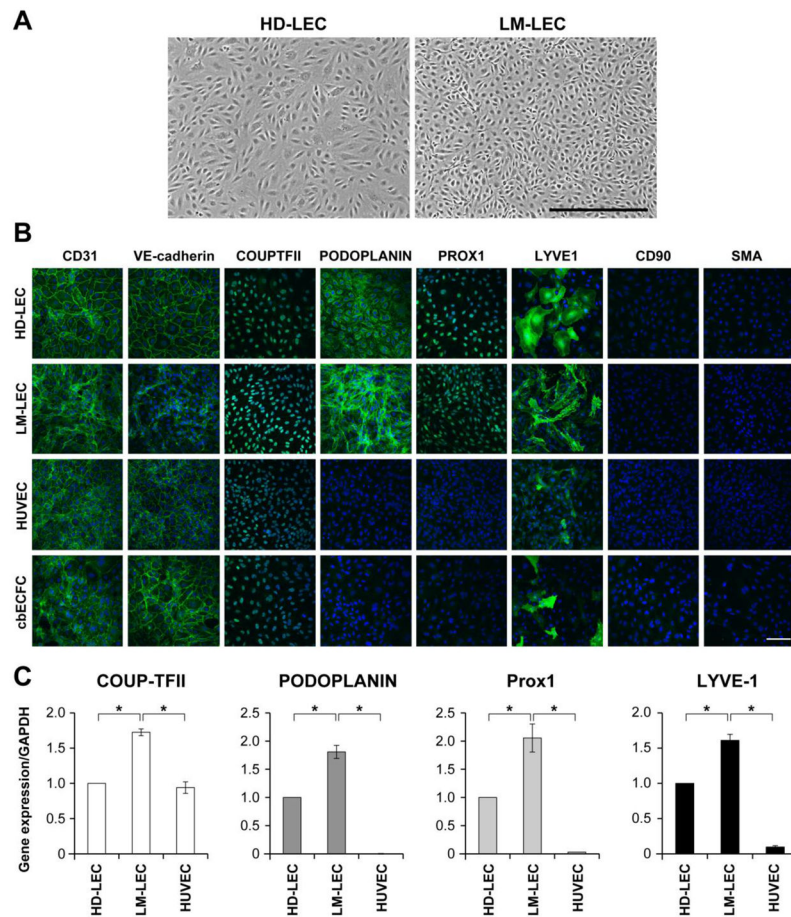


Figure 1. Characterization of LM-LEC

A. Phase image of HD-LEC and LM-LEC, in vitro. Scale bar 500µm.

Immunofluorescence staining of HD-LEC, LM-LEC, HUVEC and cbECFC for CD31, VE-Cadherin, COUPTFII, Podoplanin, Prox1, LYVE1, CD90 and αSMA. Scale bar 100µm.

C. mRNA expression levels, normalized to GAPDH, of COUPTFII, Podoplanin, Prox1, and LYVE1 in HD-LEC, LM-LEC and HUVEC, analyzed by real-time qPCR. Data expressed as mean ± SDM, * $p < 0.01$.

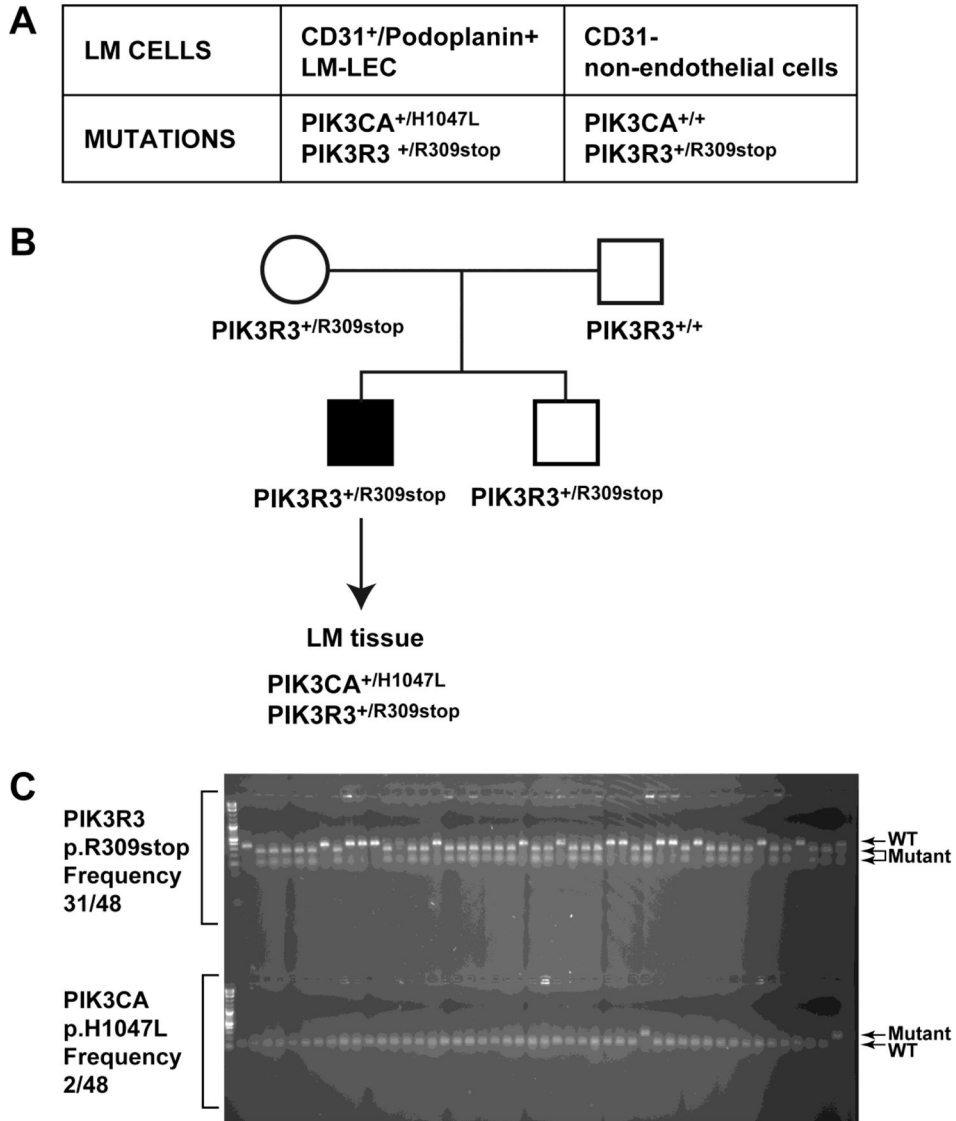


Figure 2. PIK3 mutations in LM-LECs and in LM patients' tissue
 A. Table with mutations identified in LM-LEC (CD31+/podoplanin+) and non-endothelial cells (CD31-). B. Pedigree of family of patient with LM and schematic of mutational analysis for mutations in PI3K gene in LM tissue. C. DNA subcloning from patient's LM tissue, and colony digestion with BspCNI for PIK3R3 mutation, (the mutation creates a restriction enzyme cutting site, frequency 31/48, see 2 lower bands on the gel), and digestion with BsaBI for the PIK3CA mutation (the p.H1047L base change removes a restriction site, frequency 2/48, see upper band in the gel).

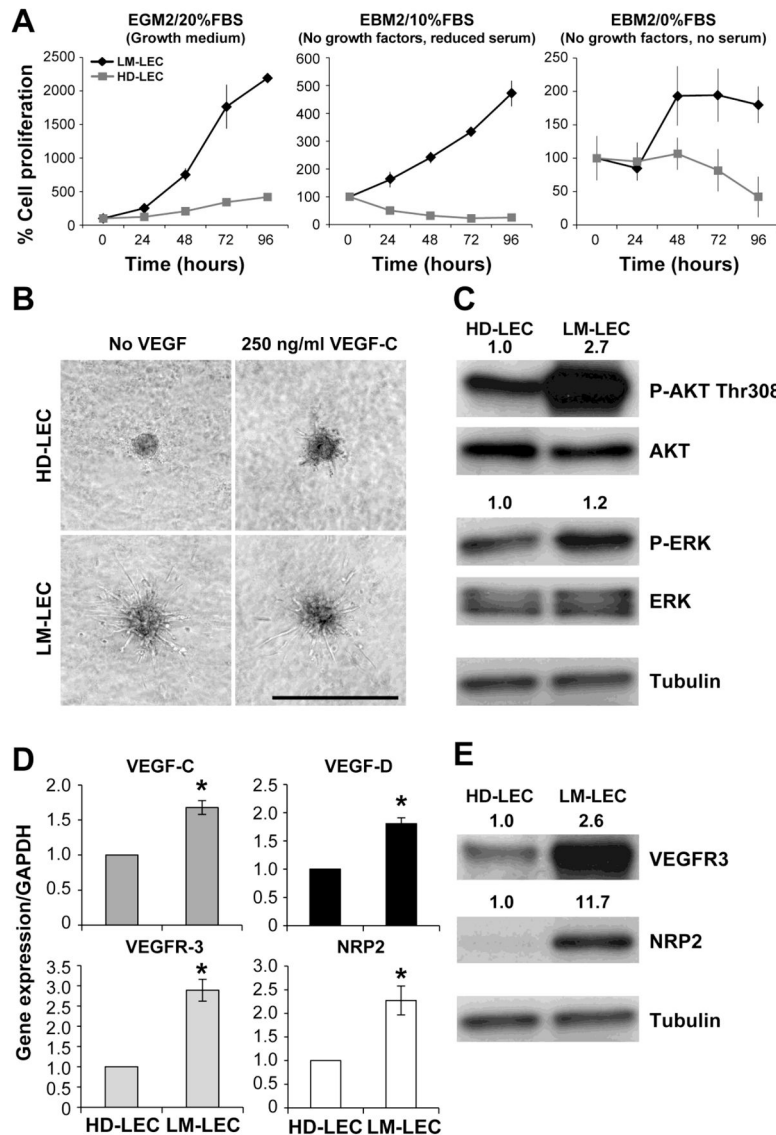


Figure 3. Angiogenic properties of LM-LEC

A. Cell proliferation evaluated at 24, 48, 72 and 96 hours for HD-LEC and LM-LEC in growth medium (EGM2/20%FBS), starvation medium (EBM2/no growth factors/10%FBS), and serum-free medium (EBM2/no growth factors/no FBS). Cell count at 24 hours after seeding was set to 100% to normalize for differences in initial adherence to the well. Data expressed as mean \pm SDM. B. Sprouting assay with HD-LEC and LM-LEC spheroids in collagen gel, after 16 hours in the absence or presence of VEGF-C 250ng/ml. Scale bar 500 μ m. C. Immunoblot of HD-LEC and LM-LEC for phosphoAKT (P-AKT) Thr308, P-ERK, and relative total AKT and total ERK. Values are normalized ratios P-AKT/AKT and P-ERK/ERK band intensities. Tubulin serves as loading control. D. mRNA expression levels, normalized to GAPDH, for VEGF-C and VEGF-D, in HD-LEC and LM-LEC, measured by real-time qPCR. Data expressed as mean \pm SDM, * $p < 0.01$. E. Immunoblot of HD-LEC and LM-LEC for VEGFR-3, NRP2 and the endothelial marker VE-Cadherin.

Values are ratios VEGFR-3/Tubulin NRP2/Tubulin and VE-Cadherin/Tubulin band intensities. Tubulin is loading control.

Author Manuscript

Author Manuscript

Author Manuscript

Author Manuscript

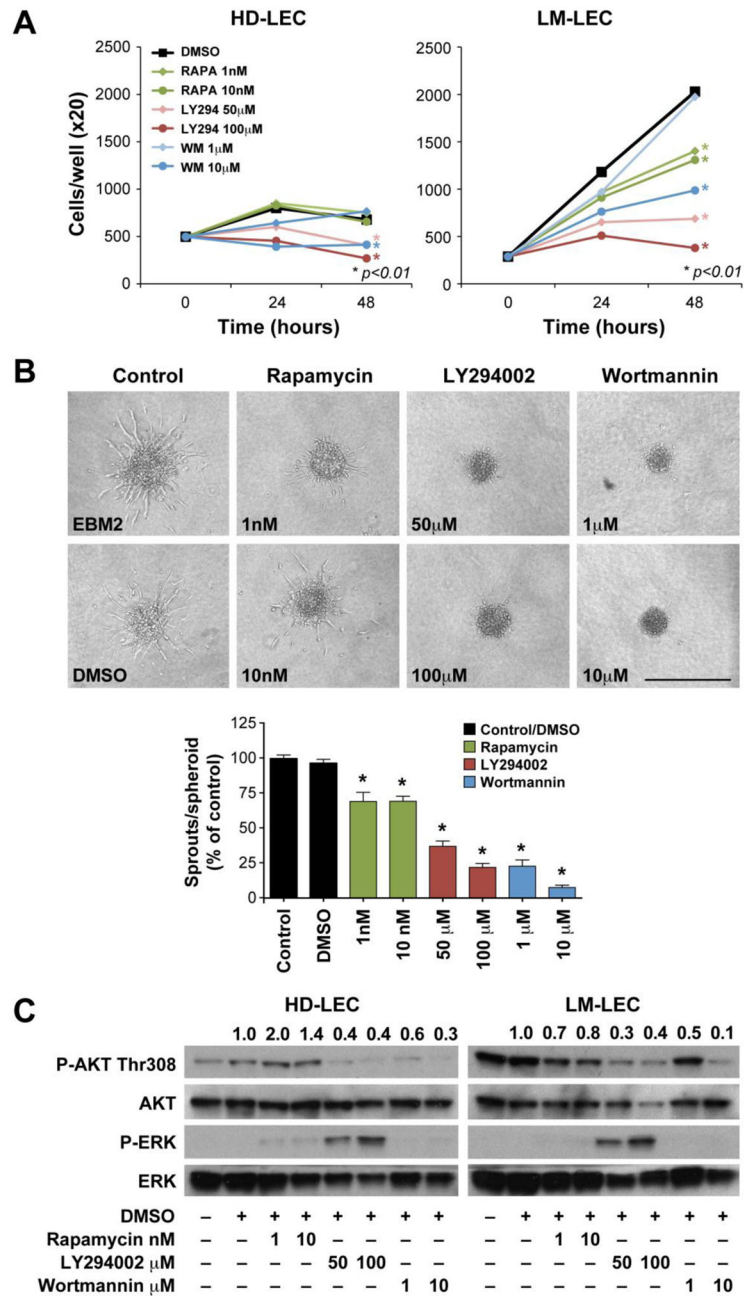


Figure 4. Effect of PI3K inhibitors and rapamycin on the pro-angiogenic properties of LM-LEC
 A. Cell proliferation evaluated at 24 and 48 hours for HD-LEC and LM-LEC treated with rapamycin (1, 10nM), LY294 (50, 100µM), and Wortmannin (1, 10 µM). Cells were grown in EBM2/10%FBS. DMSO treatment is the control. Data expressed as mean. B. HD-LEC and LM-LEC spheroids in collagen gels, after 16 hours treatment with EBM2, or EBM2 containing DMSO, rapamycin (1, 10nM), LY294 (50, 100µM), and Wortmannin (1, 10 µM). Graph illustrates quantification of EC sprouts from the spheroids, expressed in % relative to EBM2 alone. Data expressed as mean± SEM. * p 0.001. Scale bar 500µm. C. Immunoblot of HD-LEC and LM-LEC for phosphoAKT (P-AKT) Thr308, P-ERK, and relative total

AKT and ERK. Cells were treated, for 48 hours with rapamycin (1, 10nM), LY294 (50, 100µM), and Wortmannin (1, 10 µM). Values are normalized ratios P-AKT/AKT and P-ERK/ERK band intensities.

Author Manuscript

Author Manuscript

Author Manuscript

Author Manuscript